CRYSTAL GROWTH & DESIGN

Article

pubs.acs.org/crystal

Is the Fenamate Group a Polymorphophore? Contrasting the Crystal Energy Landscapes of Fenamic and Tolfenamic Acids

Published as part of the Crystal Growth & Design virtual special issue In Honor of Prof. G. R. Desiraju

Ogaga G. Uzoh,[†] Aurora J. Cruz-Cabeza,[‡] and Sarah L. Price*[,†]

[†]Department of Chemistry, University College London, 20 Gordon Street, London WC1H 0AJ, United Kingdom

[‡]Van't Hoff Institute for Molecular Sciences, University of Amsterdam, Science Park 904, 1098 XH Amsterdam, The Netherlands

Supporting Information

ABSTRACT: The concept of a polymorphophore was investigated by contrasting the crystal energy landscapes of monomorphic fenamic acid (2-(phenylamino)-benzoic acid, FA) and one of its highly polymorphic derivatives, tolfenamic acid (2-[(3-chloro-2-methylphenyl)amino]-benzoic acid, TA). The crystal energy landscapes of both molecules show that the benzoic acid $R_2^2(8)$ dimer motif is found in all low energy crystal structures, but conformational flexibility of the phenyl rings leads to a wide range of crystal structures with different packings of this dimer. Many of the observed fenamate crystal structures can overlay a significant proportion of the coordination environment with other observed or calculated structures, but the substituents of the phenyl group affect the ordering of the related low energy crystal structures. The crystal energy landscape of tolfenamic acid has several crystal structures, including the observed polymorphs, tightly clustered around the global minimum, whereas the corresponding cluster contains only the observed and a closely related structure for fenamic acid. Hence, the fenamate fragment is potentially permissive of a large number of structures because of the conformational flexibility, but the substituents determine whether a specific fenamate will be polymorphic. Thus, a polymorphophore promotes but does not guarantee polymorphism.

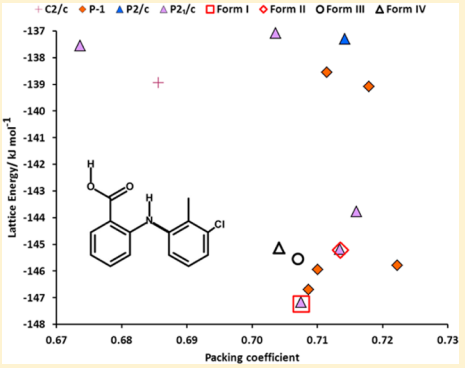

1. INTRODUCTION

Polymorphism, the occurrence of multiple crystal structures with the same chemical content, is now known to be widespread for organic molecules[1] and is of great industrial importance in the manufacture of specialty chemicals and pharmaceutical products. Relatively few systems have several polymorphs whose crystal structures and relative stabilities have been determined, the most thoroughly investigated[2] being the polymorphs of 2-[(2-nitrophenyl)amino]-3-thiophenecarbonitrile) or ROY (Figure 1), after the red, orange, and yellow color spectrum of the first six polymorphs to be reported.[3] However, there are some families of related molecules,[4,5] such as the sulphonamides,[5] ROY derivatives,[4] barbiturates,[6] carbamazepine derivatives,[7,8] and fenamates,[9] which appear to have a strong tendency for polymorphism. This has led to the concept of a polymorphophore,[4,7,9] a term first coined by Matzger[4] as a structural element that, when incorporated into a molecule, favors the formation of polymorphic crystal forms. (This is analogous to "pharmacophores" as particular structures which are particularly useful in finding new leads in drug discovery, especially when the three-dimensional (3D) structure of the receptor is unknown.[10]) The concept recognizes that there are families of molecules containing a common substructure (the polymorphophore) where many members (but not necessarily all) exhibit polymorphism. For example, removing or adding a methyl group to ROY gives molecules (Figure 1) that are also polymorphic suggesting a polymorphophore (Figure 1), though the number of related molecules is limited probably because ROY is only a precursor in the synthesis of the blockbuster drug olanzapine. The fenamates contain a proposed polymorphophore[9,11] that is related to that of ROY (Figure 1) in having a phenyl group attached via a N−H group to a further aromatic ring. The polymorphism of tolfenamic acid was seen[9] as a good test case for the notion of a polymorphophore being exemplified by the fenamate motif. In this study, we will only consider the fenamates, which conserve the hydrogen bonding groups and dominant molecular shape by having small, nonpolar substituent groups for the aromatic protons, as exemplified in Figure 1. These types of substituents might be expected to have minimal effect on the strongest intermolecular interactions, and hence either crystal packing or drug receptor binding. The term fenamate can be used to include greater variations in molecular structure such as niflumic acid, which contains aromatic nitrogen. Indeed, a thermodynamic and structural investigation of some fenamate molecular crystals included an even wider range of molecules, including

Received: May 30, 2012
Revised: July 10, 2012
Published: July 11, 2012

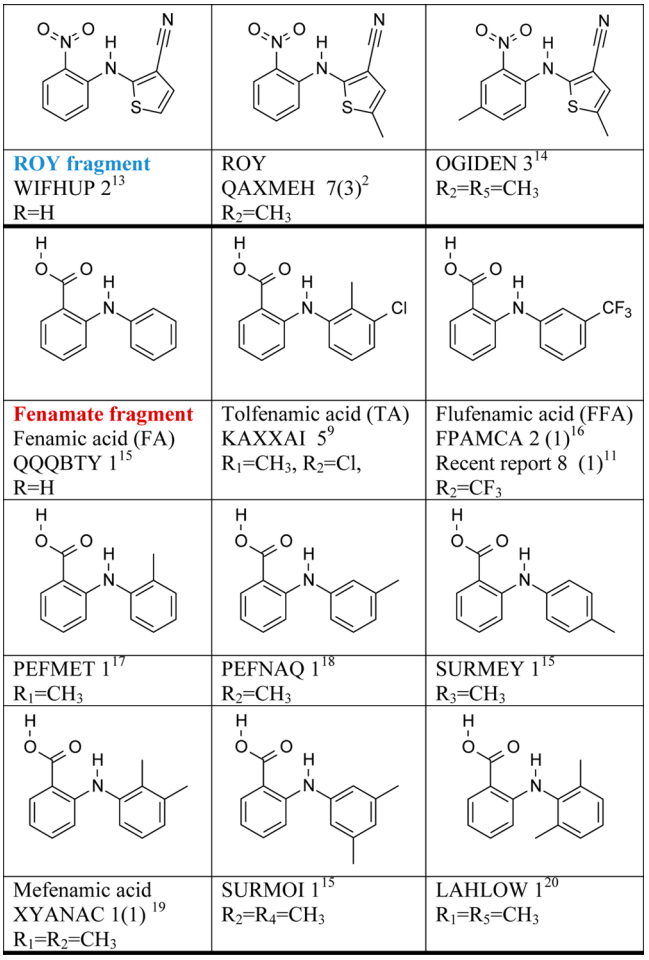

Figure 1. The polymorphophore families of ROY and fenamic acid. The number of polymorphs in the Cambridge Structural Database (CSD) follows the refcode for the specific molecule and (x) denotes the number of additional polymorphs observed but whose crystal structure is not available. The lowest two rows are fenamates whose structures are used in Table 5.

dichlofenac.[12] However, by restricting this study to fenamates in Figure 1, and their relationship to the ROY molecules, we are looking at cases where the dominant interactions that will determine the crystal or drug binding are inherent in the proposed polymorphophore.

This paper seeks to address the following questions: for a given molecular structure, is containing a polymorphophore substructure sufficient to ensure polymorphism? What role do substituents play in determining the range of polymorphs? Since the same level of polymorph screening has rarely been applied to entire families of molecules, the generation of crystal energy landscapes is a necessary addition to examining the known forms in investigating the effects of a polymorphophore. Crystal structure prediction (CSP) methods[21,22] sample a wide range of possible crystal structures in order to find the minima in the lattice energy, thus generating the crystal energy landscape.[23] This provides the experimental as well as other low energy crystal structures that are worth comparing with the known polymorphs in order to determine the types of intermolecular interactions and conformations that could be feasible for a given molecule. The method used in this study is suitable for studying flexible molecules,[24] as the ab initio charge density for the specific conformation is used in modeling the intermolecular interactions, thus representing the interplay between molecular conformation and intermolecular interactions which has been shown to be important for tolfenamic acid.[25] Conformational changes can improve the directionality of strong interactions, such as hydrogen bonding, and increase the packing density and hence the stabilization of the structure by dispersion forces. Crystal energy landscapes in which only one crystal structure is calculated to be more stable than any other by over a few kJ mol^{-1} typical of polymorphic energy differences suggest that the molecule should only be found in that global minimum structure. (Experiments or more demanding searches are needed to determine the stability relative to multicomponent forms such as hydrates,[26] solvates,[27] or cocrystals,[28,29] etc.). In most generated energy landscapes, however, there is usually a group of structures which are within the energy range of plausible polymorphs. These structures have to be qualitatively assessed to see whether the barriers between the different structures are so low that thermal motion in the crystal or molecular rearrangement during nucleation and growth will ensure that only the most thermodynamically stable structure is seen. (Closely related structures may also give rise to disorder[30,31] or plastic phases[32] at higher temperatures.) The

Table 1. Experimental Data of the Known Forms of Fenamic and Tolfenamic Acid[a]

REFCODE (form)	space group	Z'	ξ_1[b] (°)	T[c] (K)	ΔH_{fus} kJ mol^{-1}	T_m[d] (K)
			FA			
QQQBTY02	$P\bar{1}$	2	47.21, 70.45	283−303[15]		
			TA			
KAXXAI01(I)	$P2_1/c$	1	107.74		39.37	486.25−488.6
				110	42.50	484.05[35]
					41.0 ± 0.5	484.18 ± 0.2[36]
					41.27	485.85[37]
KAXXAI(II)	$P2_1/n$	1	42.23		38.7	486.67
				110	48.40	487.65[35]
					49.0 ± 0.5	485.78 ± 0.2[36]
					42.40	414.95[37]
KAXXAI02 (III)	$P2_1/c$	2	44.19, 57.64	85		
KAXXAI03 (IV)	$P\bar{1}$	3	67.34, 57.58, 47.84	85	31.88	
KAXXAI04 (V)	$P\bar{1}$	1	55.62	85		

[a]Crystal structures and ΔH_{fus} values are taken from ref 9 unless otherwise specified. [b]The most widely varying torsion angle, ξ_1, is defined in Figure 3. [c]Temperature of crystal structure determination. [d]Melting temperature.

dx.doi.org/10.1021/cg3007348 | Cryst. Growth Des. 2012, 12, 4230−4239

crystal energy landscape may suggest that alternatives to the known structures could be found as either more stable or kinetically trapped, metastable polymorphs. In this case, the calculations can complement experimental screening[33] by suggesting alternative methods,[34] such as a templating, to produce new polymorphs.[8] Thus a comparison of the crystal energy landscapes of the most basic fenamate molecule, fenamic acid (FA) with the most extensively experimentally studied fenamate; tolfenamic acid (TA) (Figure 1) allows an investigation of the concept of a polymorphophore.

TA is a nonsteroidal anti-inflammatory drug that possesses at least five polymorphs, forms I–V.[9,35] Unlike ROY, the polymorphs of TA vary in the number of molecules in the asymmetric unit, Z' (Table 1). The variation of colors observed for form I (colorless) and II (yellow) is due to the conformational difference, as observed for ROY.[2,4] There are three undisputedly metastable polymorphs, including form V whose disorder is analyzed further in the Supporting Information. The evidence for the relative stability of forms I and II (Table 1) is discussed further in the Supporting Information, and form II is probably the most stable polymorph at 0 K. Fenamic acid has just one known form,[15] which has two molecules in its asymmetric unit.

2. COMPUTATIONAL METHODS

The crystal energy landscapes[23] of fenamic and tolfenamic acids were calculated by a methodology[38] adapted from that used for the highly flexible molecule XX in the fifth blind test of crystal structure prediction,[22] which uses an approximate conformational energy surface in the initial search stage.

Isolated molecule ab initio calculations were performed on FA and TA using GAUSSIAN 03[39] at the PBE0/6-31G+(d) level of theory to provide a relaxed conformational scan of the main torsion angle, ξ_1 (Figure 2). This was complemented with a Conquest search of the

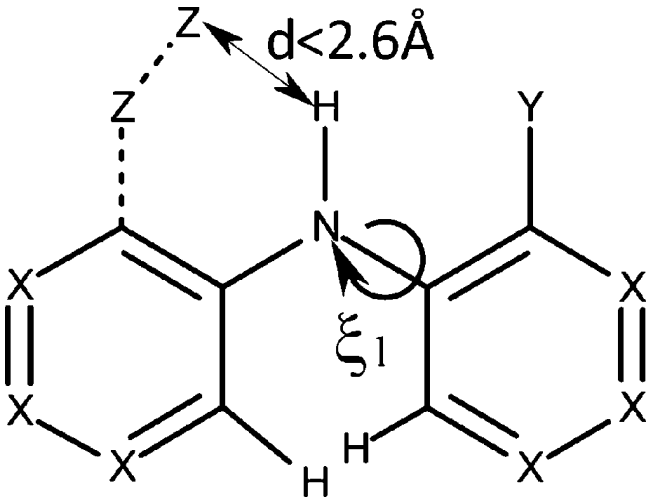

Figure 2. Query fragment and the torsion angle ξ_1 measured in the Conquest[41] survey of the CSD structures. There were 131 organic structures where Y = H, and 94 where Y ≠ H.

Cambridge Structural Database (CSD)[40] for the crystal structures containing the molecular fragment in Figure 2, in order to see the variation in ξ_1 when there is an internal hydrogen bond (Z···H < 2.6 Å) that constrains part of the molecule to planarity.

The crystal energy landscapes of TA and FA were generated in four steps, with increasing quality of the methods to estimate the conformational energy penalty ΔE_{intra} and the intermolecular contribution U_{inter} to the lattice energy, $E_{latt} = U_{inter} + \Delta E_{intra}$.

Step 1. Crystal structures with $Z' = 1$ were generated in 15 common space groups: $P1$, $P\bar{1}$, $P2_1$, $P2_1/c$, $P2_12_12$, $P2_12_12_1$, $Pna2_1$, $Pca2_1$, $Pbca$, $Pbcn$, $C2/c$, Cc, $C2$, Pc, and $P2/c$, using CrystalPredictor.[42] The search used extrapolated the grids for atomic charges and intramolecular energy ΔE_{intra}, which had been calculated as a function of ξ_1 using GAMESS[43] at the MP2/6-31G(d,p) level of theory (single point calculation), after the molecular geometries were optimized at the HF/6-31G(d,p) level. The intermolecular contributions to the lattice energy were calculated from the atomic charges and the William's exp-6 repulsion-dispersion potential.[44] The CrystalPredictor program produced over 150 000 lattice energy minima for each molecule, but only about 20 000 were unique.

Step 2. Single point isolated molecule ab initio calculations were carried out on the conformation in each of the generated crystal structures, using GAUSSIAN[39] at the PBE0/6-31G(d,p) level of theory, to improve the estimate of ΔE_{intra} and provide the atomic multipoles, by distributed multipole analysis[45] using GDMA. The crystal structures were reoptimized, keeping the molecule rigid, using DMACRYS[46] with the lattice energy U_{inter} calculated from the distributed multipoles and the FIT parametrization[47−49] of the exp-6 atom−atom repulsion-dispersion potential.

Step 3. The most stable and unique crystal structures were reminimized, allowing six or seven conformational degrees of freedom for FA and TA, respectively (Figure 3), to change as well as the crystal

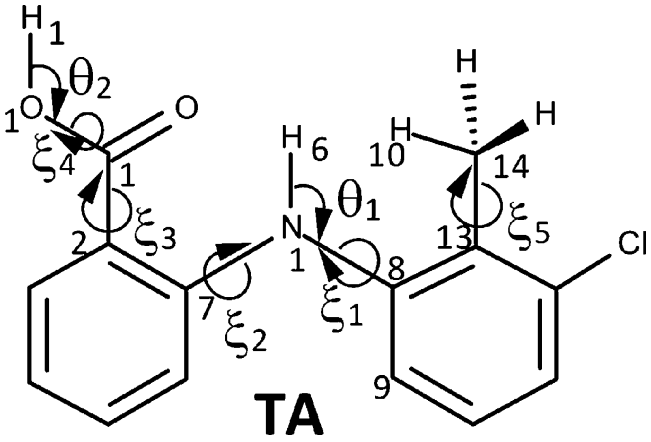

Figure 3. The degrees of freedom optimized by CrystalOptimizer for crystal structures of FA and TA ($\xi_1 \equiv C_7–N_1–C_8–C_9$, $\xi_2 \equiv C_2–C_7–N_1–C_8$, $\xi_3 \equiv O_1–C_1–C_2–C_7$, $\xi_4 \equiv H_1–O_1–C_1–C_2$, and $\xi_5 \equiv C_8–C_{13}–C_{14}–H_{10}$, $\theta_1 \equiv H_6–N_1–C_8$, $\theta_2 \equiv H_1–O_1–C_1$).

structure, using CrystalOptimizer[50,51] and calculating ΔE_{intra} and the distributed multipoles at the PBE0/6-31+G(d) level of theory for the isolated molecule.

Step 4. Finally, the effect of the crystal environment was estimated using a polarizable continuum model (PCM)[52] obtained by calculating the wave function of the molecular structure in a dielectric of $\varepsilon = 3$ (typical of molecular organic crystals),[53] as implemented in Gaussian03. The crystal structures were then reminimized using the distributed multipoles calculated in the PCM environment while keeping the molecule rigid, and the resulting U_{inter} was combined with the ΔE_{intra} to evaluate the final lattice energies. The CSP generated crystal structures for FA are labeled #*x*FA_*y*, where *x* is the final energy ordering and *y* is the ordering after the CrystalPredictor stage, so a comparison of *x* and *y* shows the extent of reranking by increasing the accuracy of the lattice energy model.

Because of the complexity of generating $Z' > 1$ crystal energy landscapes for flexible molecules, this search can only generate the observed $Z' = 1$ ordered forms (I and II of TA). Analogous CrystalOptimizer and PCM calculations were performed starting from the experimental crystal structures of TA and FA, to allow comparison with the $Z' > 1$ structures FA form I and TA forms III and IV. Form V of TA is a $Z' = 1$ structure in $P\bar{1}$ showing positional disorder of two

dx.doi.org/10.1021/cg3007348 | Cryst. Growth Des. 2012, 12, 4230−4239

different conformers in the asymmetric unit cell. In order to investigate this structure, three different form V $Z = 2$ ordered models were built and evaluated by combining the two possible conformers in the $Z = 2$ $P\bar{1}$ unit cell (see Supporting Information).

The experimental crystal structures, the corresponding lattice energy minima, and the structures on the crystal energy landscapes were compared using the Crystal Packing Similarity[54] module implemented in Mercury.[55] This crystal structure similarity tool returns the highest number of molecules n (where $n \leq 15$) that can be overlaid between two different structures when all non-hydrogen atom−atom distances are within a 20% distance tolerance and angles within 20°. The calculated rmsd_n is the root-mean-square deviation of all non-hydrogen atom positions in the clusters of n molecules. The program allows for comparisons of crystal structures of different molecules with the rmsd_n being calculated from only the common non-hydrogen atoms. This Crystal Packing Similarity calculation determines the similarity in the coordination environment of the two crystal structures, rather than the crystallographic cell.

3. RESULTS

3.1. Conformations in Known Crystal Structures. The overlay of the conformers of fenamic and tolfenamic acid in the experimental crystal structures (Figure 4) illustrates that the

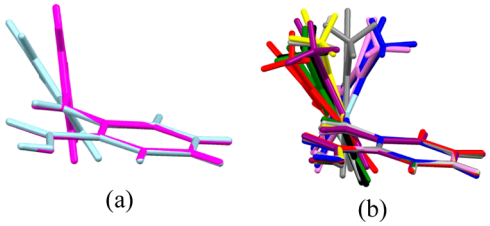

Figure 4. Overlay of the experimental conformers of (a) fenamic acid and (b) tolfenamic acid, viewed with the overlaid benzoic acid fragment horizontal. FA: QQQBTY02 ($Z' = 2$; light blue and magenta). TA: KAXXAI01 (Form I; $Z' = 1$; blue), KAXXAI (Form II; $Z' = 1$; red), KAXXAI02 (Form III; $Z' = 2$; green and purple), KAXXAI03 (Form IV; $Z' = 3$; yellow, brown (obscured by yellow) and black), KAXXAI04 (Form V; $Z' = 1$; disordered on both sites (Supporting Information); violet and gray).

main variation in conformation is the torsion angle ξ_1. The two most stable polymorphs of TA, form I and form II (Figure 4), have the largest difference in ξ_1. The acid and N−H groups are coplanar with the ξ_2 torsion angle being approximately zero, concordant with the intramolecular hydrogen bond producing a sharp increase in energy for varying this angle (Supporting Information).

The conformational potential energy surface of isolated TA and FA molecules (Figure 5a) is similar for a wide range of conformations around those depicted in Figure 4, but differs as the bulky methyl substituent of TA approaches the benzoic acid ring (Figure 5a). For FA, the energy penalty for conformational change, ΔE_{intra}, is less than 6 kJ mol^{-1} over all possible conformations, whereas for TA there is a conformational region that is far too high in energy to occur in crystal structures. The observed conformations of FA and TA in their crystal structures correspond to low energy isolated molecule conformations (Figure 5a), with a relative intramolecular energy, ΔE_{intra}, of less than 3 kJ mol^{-1}. The conformational profile for TA is in qualitative agreement with that calculated by other high quality ab initio methods (Supporting Information Figure S3), but is quantitatively affected by the subtle balance between intramolecular dispersion and intramolecular basis set superposition error.[56] Other studies also suggest that the

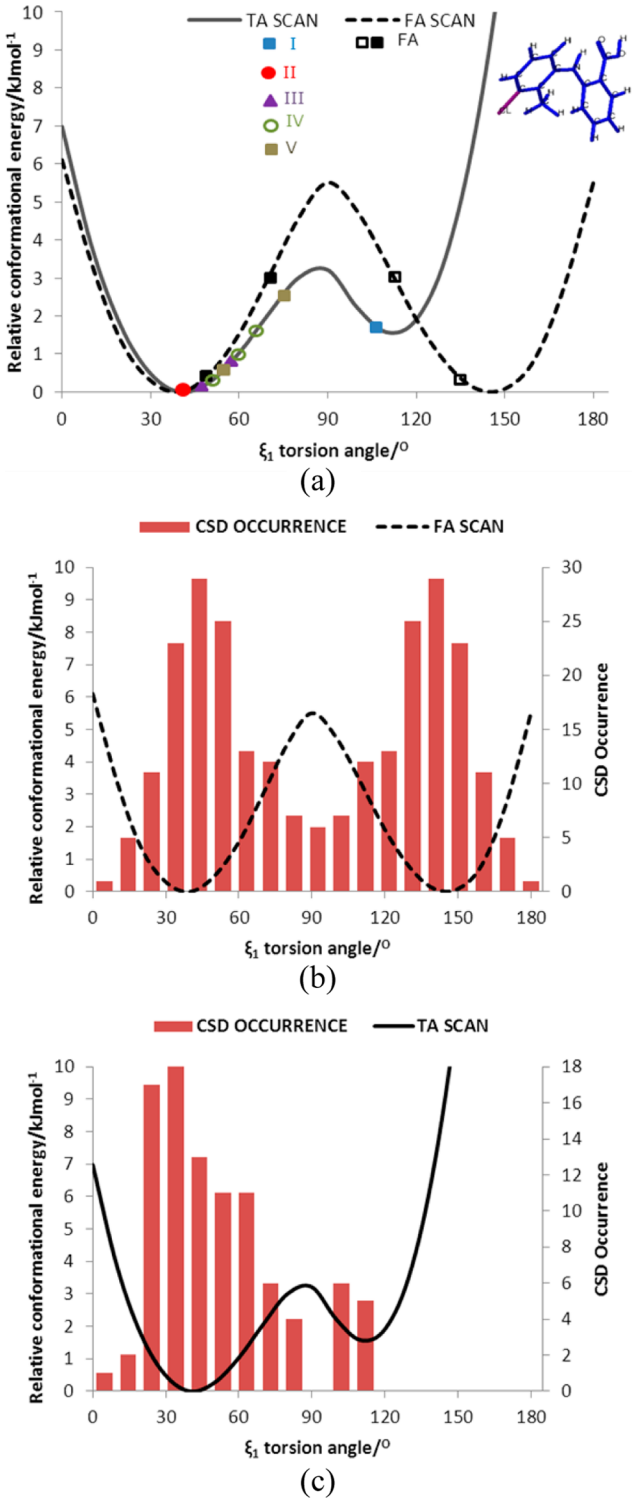

Figure 5. The relative conformational energy as a function of the ξ_1 torsion angle of fenamic (FA) and tolfenamic (TA) acids, calculated in a relaxed scan at the PBE0/6-31+G(d) level of theory. (a) Includes the experimental values of ξ_1 marked for TA and FA, with the symmetry equivalent FA conformations denoted by open black squares and an inset diagram showing the steric hindrance for TA in the high-energy region. (b) a histogram of the number of the 131 crystal structures in the CSD found in the search (Figure 2) with Y = H binned by torsion angle, including symmetry equivalences; (c) the torsion angle distribution in the 94 CSD structures with Y ≠ H.

dx.doi.org/10.1021/cg3007348 | Cryst. Growth Des. 2012, 12, 4230−4239

barriers to conformational change would be even lower in solvents from calculations in a dielectric continuum simulating CCl_4 and methanol.[25]

The crystal structures in the CSD that contain our search criterion (Figure 2) also show the same preference for the lower energy conformations,; that is, the distribution maxima coincide with the conformational minima (Figure 5b,c), with very few structures having the two rings near coplanar or perpendicular (ξ_1 = 0, 90°) around the local maxima in the conformational energy scans. For the Y = H search, because both ortho substituents are hydrogen atoms, two torsion angle values arise per conformation in a crystal structure (one value between 0 and 90° and the second value between 90° and 180°), giving a symmetric plot (Figure 5b). For Y ≠ H, on the other hand, each structure has only one torsion angle value, and the distribution Figure 5c is not symmetric, reflecting the steric hindrance of the ortho substituent.

3.2. Experimental Crystal Structures. The known polymorphs of TA and FA show some similarities (Table 2),

Table 2. Quantification[a] of the Similarities of Fenamic and Tolfenamic Acid Crystal Structures Showing the Packing Similarity (rmsd$_n$) and Powder X-ray Diffraction (PXRD) Similarity[57]

	n(rmsd$_n$/Å)				
	FA	**TA(I)**	**TA(II)**	**TA(III)**	**TA(IV)**
FA	-	**6**(0.66)	**2**(0.48)	**3**(0.74)	**5**(1.08)
TA(I)	0.78	-	**1**(0.87)	**3**(0.78)	**3**(1.07)
TA(II)	0.85	0.86	-	**2**(0.77)	**2**(0.74)
TA(III)	0.78	0.83	0.90	-	**11**(0.45)
TA(IV)	0.78	0.84	0.92	0.98	-
TA(V)	0.86	0.89	0.93	0.91	0.93
	PXRD Similarity				

[a]The bold numbers indicate the number of molecules, n, that match within distance and angle tolerances of 20% and 20° respectively with the rmsd$_n$ values in brackets.

as all are based on the hydrogen-bonded dimer (Figure 6a). Form II had the most distinctive packing (Figure 6b) as well as conformation (Figure 4b) and is the only structure with a short contact involving the chlorine atom and the aromatic ring. The most striking result from Table 2 is the similarity between the metastable forms III and IV, where 11 molecules can be overlaid (Figure 6c). The two independent molecules in form III have similar conformations to two of the three independent molecules in form IV. The polymorphs have sufficiently similar simulated powder patterns to have a PXRD similarity measure in the gray area between polymorphism and redeterminations[58] and so exemplify issues in defining polymorphism.[59,60]

3.3. Validation of Computational Model. The computational model is able to reproduce all ordered crystal structures satisfactorily as minima in the lattice energy (Table 3), with these static 0 K structures overlaying the finite temperature crystal structures with similar accuracy. The range of lattice energies is less than 2 kJ mol^{-1}, consistent with the small energy range expected for such polymorphs and the thermodynamic data (Table 1). Form I is the most stable at 0 K, in disagreement with the monotropic relationship between forms I and II determined by DSC measurements[35,36] and other data (Supporting Information). Forms III and IV are metastable and very close in energy to form II. Of the three form V Z = 2 ordered model crystal structures, two have a

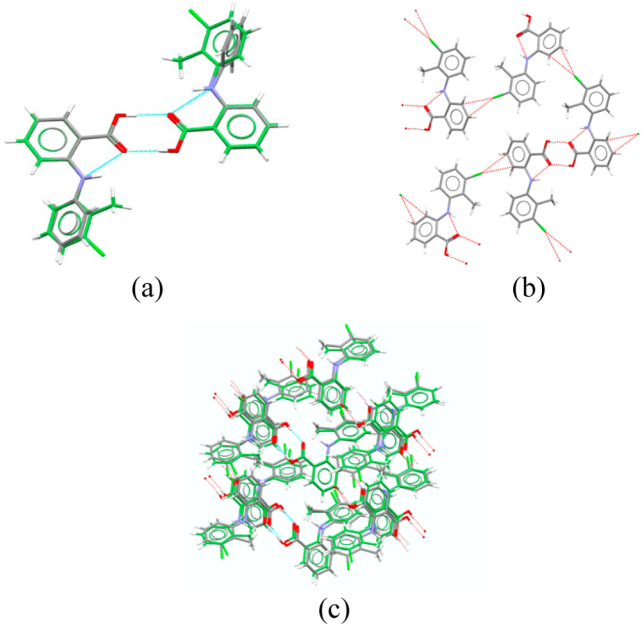

Figure 6. Features of the experimental crystal structures: (a) the hydrogen-bonded dimer motif found in all structures with variations in the phenyl ring orientations (ξ_1). The specific illustration is the packing similarity between FA (QQQBTY02) and TA form II (KAXXAI). (b) The unique packing for TA form II with short contacts between chlorine and the aromatic ring. (c) Crystal Packing Similarity between form III and form IV of TA showing the 11 molecule overlay, which includes only two dimers.

nearby lattice energy minimum, but all are quite high in energy. The disordered structure is therefore likely to be more complex than a combination of these structures, but a full symmetry adapted ensemble study of a large supercell[31,61] is not appropriate without more detailed experimental studies.

3.4. The Crystal Energy Landscapes. The known forms of fenamic and tolfenamic acid are at, or close to, the global minimum on their crystal energy landscape (Figure 7), which generated all the known Z' = 1 ordered polymorphs. The crystal energy landscapes of FA and TA are similar in that there is an energy gap of approximately 2 kJ mol^{-1} between the global minimum cluster and other structures, though the cluster of low energy structures is far larger for TA. Although this suggests that TA will be more polymorphic than FA, it is necessary to compare the structures to see if it is plausible that they could crystallize as distinct polymorphs, allowing for thermal motion at crystallization temperatures. All the crystal structures whose energies are plotted in Figure 7 (and are tabulated in Supporting Information Tables S2 and S3) contain the carboxylic acid dimer (Figure 6a) though the orientation of the phenyl substituents can differ so markedly that this dimer does not always satisfy the distance criterion to be overlaid by the default Crystal Packing Similarity comparison. Hence, the structures are distinguished by the packing of the aromatic rings, and it is necessary to qualitatively assess the barrier to rearrangement of the molecules to a more stable form.

The lowest energy hypothetical structure on the crystal energy landscape for FA is a Z' = 1 structure (#1FA_22) that is very similar in density and lattice energy to the only known experimental Z' = 2 form (Figure 7a), with a PXRD similarity of 0.85. #1FA_22 overlays five molecules (Figure 8a) with the experimental form and matches the conformation of one of the

dx.doi.org/10.1021/cg3007348 | Cryst. Growth Des. 2012, 12, 4230−4239

Table 3. Comparison of the Lattice Energy Minimum with the Experimental Structure, Used As a Starting Point for the Final Lattice Energy Model (PBE0/6-31+G(d) PCM), for the Ordered Structures of FA and TA[a]

	space group	ρ (g cm^{-3})	E_{latt} (kJ mol^{-1})	$a\ b\ c$ (Å)	$\alpha\ \beta\ \gamma$ (°)	rmsd$_n$ (Å)
			FA			
Expt	$P\bar{1}$	1.33		8.08; 9.81; 14.04	85.96; 88.64; 73.45	
Opt	$P\bar{1}$	1.34	−136.63	8.48; 9.91; 13.33	90.94; 88.16; 71.30	0.46
			TA			
Expt I	$P2_1/c$	1.44		4.83; 32.13; 8.04	90.00;104.88; 90.00	
Opt I	$P2_1/c$	1.39	−147.24	4.86; 31.54; 8.32	90.00;102.00; 90.00	0.33
Expt II	$P2_1/n$	1.45		3.84; 22.00; 14.21	90.00; 94.11; 90.00	
Opt II	$P2_1/n$	1.41	−145.21	3.86; 22.06; 14.60	90.00; 96.21; 90.00	0.26
Expt III	$P2_1/c$	1.44		7.64; 11.31; 28.07	90.00; 93.03; 90.00	
Opt III	$P2_1/c$	1.39	−145.55	7.83; 11.64; 27.48	90.00; 93.32; 90.00	0.30
Expt IV	$P\bar{1}$	1.44		7.52; 14.33; 17.59	90.00; 103.68; 90.00	
Opt IV	$P\bar{1}$	1.38	−145.14	7.65; 14.00; 18.28	102.56; 99.32; 91.52	0.37(14)
Expt V	$P\bar{1}$	1.44		7.65; 9.02; 9.42	107.40; 92.06; 101.70	
Opt V_a	$P\bar{1}$	1.38	−139.54	7.67; 9.19; 9.61	107.56; 93.99; 100.87	0.21
Opt V_b	$P\bar{1}$	1.37	−141.77	6.78; 10.77; 8.97	92.75; 85.03; 103.48	0.89(6)
Opt V_c	$P\bar{1}$	1.39	−144.37	7.68; 9.28; 9.49	106.95; 92.51; 102.49	0.19

[a]The three form V $Z = 2$ model structures derived from the disorder components of TA (Supporting Information) are also compared with the starting model. rmsd$_n$ corresponds to $n = 15$ unless (n) is given.

independent molecules (Figure 8b). The difference between these two structures lies in the packing of the layers, a difference which is seen in many polymorphs, such as progesterone.[63]

There is a significant energy gap between the experimental and lowest energy $Z' = 1$ structure and the other structures generated for FA (Figure 7a). What is remarkable is that this gap is between two hypothetical structures, which only differ in the packing of the layers, having a 12 molecule overlay. The lower energy structure (#1FA_22) has more close contacts and a higher packing coefficient. The second most stable hypothetical structure (#2FA_2) is also closely related to the experimental structure, in which half the molecules have changed the phenyl torsion angle to a less stable conformation, changing the $\pi-\pi$ stacking with the phenyl ring in the neighboring molecule to a herringbone (C−H···π) interaction (Figure 9b,c). Thus, there are two different ways (Figure 9) in which #2FA_2 can gain 2 kJ mol^{-1} stabilization. This relationship between the two most stable structures (#1FA_22 and experiment) means that it may be very difficult to produce the $Z' = 1$ structure as a polymorph. This is clearly a case where a $Z' = 1$ and $Z' = 2$ structures are very close in energy, and being related (via #2FA_2), it is difficult to establish whether the observed form is a "crystal on the way"[64] trapped by a barrier from rearranging to the $Z' = 1$ form, or the more stable structure.[65]

For tolfenamic acid, the crystal energy landscape successfully found the $Z' = 1$ polymorphs, forms II and I, as the first and fifth most stable crystal structures, within 2 kJ mol^{-1} of the global minimum (Figure 7b), and provided a good reproduction of the experimental crystal structures (Figure 10 and Table 3). There are four other structures, which are competitive in lattice energy with the known metastable forms. These crystal structures also have some similarities in their packing to the known forms of TA (Table 4), some being more similar to the form V $Z = 2$ model structures constructed from the disorder components of TA than the other polymorphs (contrast Tables 2 and 4). Some of the similarities in structure (Table 5) with the other fenamates in Table 1 are even more striking. One of the computed structures #6TA_82 matches 15 molecules of SURMOI (Table 1), suggesting that crystals of this dimethyl substituted molecule might template the nucleation of a novel polymorph of TA.

There are further marked similarities between the structures on the crystal energy landscapes of FA and TA (Supporting Information Figure S8). The common clusters produced by the similarity overlays between different fenamates usually have the differing substituents in the exterior region where there is no overlay of the coordinating molecule, consistent with the substituents causing the difference in the packing. This is in marked contrast to the large common cluster between forms III and IV of TA (Figure 6c), where the packing of the aromatic rings is similar.

Some fenamate crystal structures are specific to the molecule. One observed example (Table 5) is the FPAMCA polymorph of flufenamic acid. This molecule has recently set a new record[11] for a polymorphic compound with solved structures, through the use of polymer-induced heteronucleation and solid−solid transformations. The new structures are all based on the carboxylic acid dimer, with some having more similarity to the TA and FA low energy structures (Supporting Information Table S3). The specific substituents will affect the range of packings of the aromatic rings: for example the low energy unobserved structures of FA, which are based on a planar conformation of the entire molecule (Supporting Information Figure S8) are probably also specific to FA, as the lowest energy crystal structure of TA with a planar molecule is 14 kJ mol^{-1} above the global minimum structure. This energy difference is due to the substituent intermolecular interactions destabilizing the structures containing planar molecules since the intramolecular energy penalty, ΔE_{intra}, for this planar conformation is similar for FA and TA (~6 kJ mol^{-1}, Figure 5).

4. DISCUSSION

The concept of a polymorphophore as a structural fragment that promotes polymorphism needs careful consideration given how the recent progress in polymorphism research[59] has shown that polymorphism is quite widespread. To be useful, the term polymorphophore must be promoting crystalline polymorphs and not include structural features that cause difficulty in

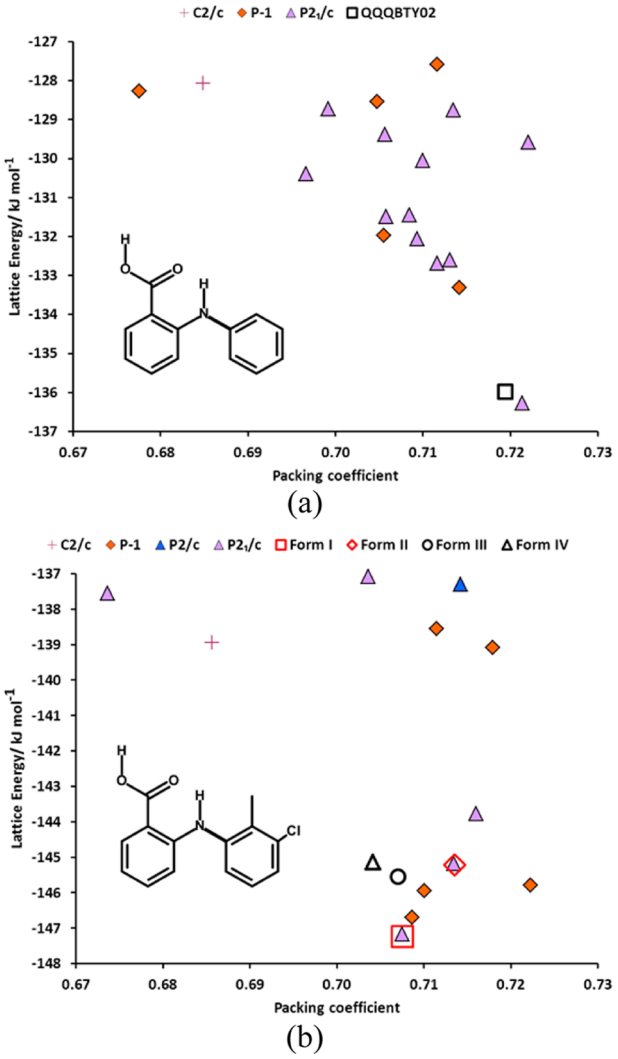

Figure 7. Crystal energy landscape of (a) fenamic acid and (b) tolfenamic acid. Each symbol represents a crystal structure of the specified space group, which is a minimum in the lattice energy (calculated within the polarizable continuum). The open symbols correspond to the minima starting from the experimental structures (Table 3). The packing coefficient is the proportion of the cell volume occupied by the molecule,[62] calculated using a grid spacing of 0.1 Å.

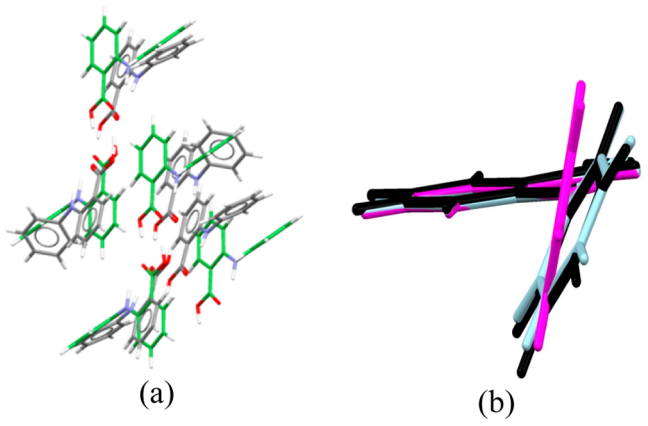

Figure 8. (a) Overlay of the only known form of FA (gray), and the most stable structure on the $Z' = 1$ crystal energy landscape (Figure 7a) #1FA_22 (green) with an $rmsd_5$ value of 1.75 Å. (b) Overlay of the conformers of form I (pink and light blue) and #1FA_22 (black).

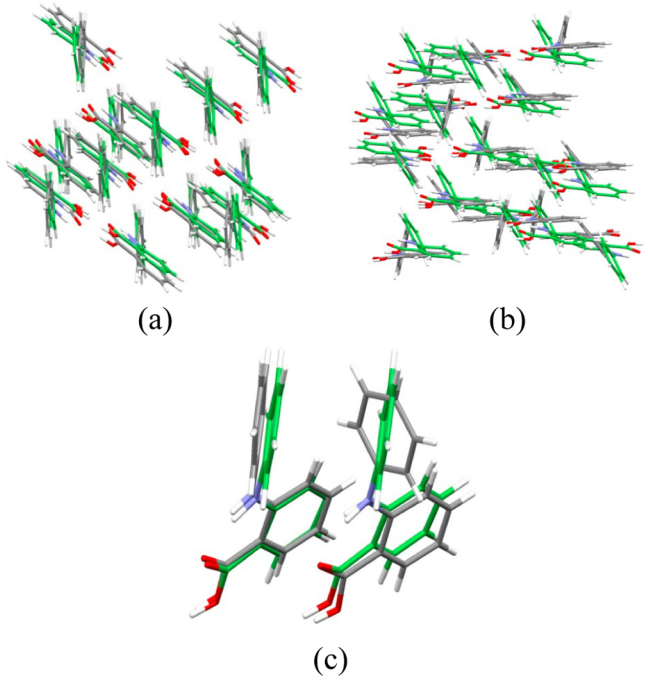

Figure 9. (a) Overlay of the two most stable hypothetical crystal structures on the crystal energy landscape; global minimum #1FA_22 (gray), and #2FA_2 (green) with ΔE_{latt} = 2.0 kJ mol^{-1}. The crystal structures overlay 12 molecules with $rmsd_{12}$ of 0.51 Å and the conformations have an $rmsd_1$ of 0.09 Å. (b) Overlay of #2FA_2 (green) and the experimental crystal structure of FA (gray) with a $rmsd_{15}$ of 1.23 Å, obtained with a distance and angle tolerance of 50% and 50°. (c) Overlay of the two independent molecules in the experimental structure (gray) with #2FA_2 (green).

crystallizing, for example, promoting the stability of amorphous forms. The fenamate group satisfies this, as the phenyl rings are expected to lead to poor glass-forming ability according to a recent study.[66] A polymorphophore is also more specific than general statements about conformational flexibility and multiple hydrogen bonding possibilities being molecular properties that may favor polymorphism.[67]

Comparison of the crystal energy landscapes of FA and TA shows that the low energy structures all have the same hydrogen bonding motif, the $R_2^2(8)$ dimer. The low energy crystal structures differ in the packing of the phenyl rings which stick out on either side of this (approximately planar) acid dimer building block (Figure 6a). The torsional flexibility allows this dimer to adopt a variety of shapes, allowing the phenyl rings to pack with themselves and the benzoic acid dimer in a variety of ways. Once the aromatic rings have interdigitated, there is a large barrier to rearranging to a very different packing, and the polymorphs may be long-lived with the torsion angles varying slightly to optimize the packing for a given structure (as clearly seen for TA). Thus, the strength of the interactions between the aromatic groups and the barriers to rearrangement are sufficient to produce different crystalline polymorphs. Hence, the fenamate fragment does qualify as a polymorphophore in that the dimeric unit can pack in a variety of ways with different torsional rotations of the phenyl groups.

However, the comparison between tolfenamic and fenamic acids clearly shows that the substituents play the major role in determining the possible packings and relative energies. The steric effects of the chloro and methyl substituents dominate

dx.doi.org/10.1021/cg3007348 | *Cryst. Growth Des.* 2012, 12, 4230−4239

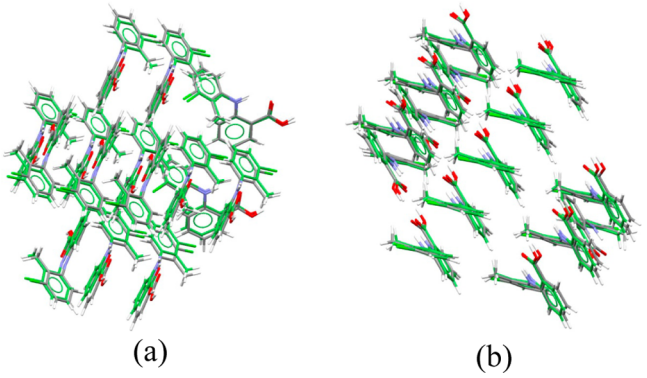

Figure 10. The overlay of the experimental $Z' = 1$ crystal structures (gray) of TA with the closest structure found in the search (green) (a) Form I and #1TA_8 overlaid with an $rmsd_{15}$ value of 0.32 Å (b) Form II and #5TA_38 overlaid with an $rmsd_{15}$ value of 0.26 Å.

Table 4. Crystal Packing Similarity Calculations of the Known Forms of TA and Unobserved Thermodynamically Competitive Crystal Structures[a]

	n ($rmsd_n$/Å)			
	#2TA_15	#3TA_876	#4TA_6243	#6TA_82
KAXXAI	1(0.95)	**4(0.33)**	1(0.88)	**9(0.43)**
KAXXAI01	1(0.49)	1(0.96)	**5(1.32)**	1(0.90)
KAXXAI02	2(0.87)	3(1.08)	2(0.95)	3(0.59)
KAXXAI03	2(0.83)	3(0.81)	3(2.55)	3(0.81)
KAXXAI04_a	**4(1.25)**	1(0.92)	3(0.16)	1(0.86)
KAXXAI04_b	**4(1.28)**	3(0.92)	**6(1.07)**	2(0.69)
KAXXAI04_c	1(0.13)	2(1.20)	**4(1.05)**	1(0.59)

[a]The similarity is given in the form $n(rmsd_n)$ where n is the number of molecules overlaid, while the value in bracket is the $rmsd_n$ overlay. Structures showing the highest similarity are highlighted.

the range of crystal packings, for example, destabilizing the packings of a planar dimer motif that are quite favorable for FA. Introducing these substituents has minimal effect on the hierarchy of intermolecular interactions: the chloro-aromatic interaction seen in TA form II (Figure 6b) is not drastically stabilizing. However, the observation of more metastable forms of TA is clearly a function of the problems of packing the substituents (Figure 6c). The packing similarity calculations between FA, TA (Table 4), and related fenamates (Table 5) clearly shows that there are many different clusters of the dimeric units that can be in common between structures of different molecules, but the variation in phenyl substituents affects how these clusters pack and their relative energies.

The fenamate crystal energy landscapes clearly show a far greater degree of similarity between the low energy structures than has been seen between isomers of near rigid molecules, such as the chlorobenzenes[68] and fluoroisatins,[69] or for differences in substituents in the 5-substitued uracils,[70] where the relative energies of the crystals with different uracil hydrogen-bonded motifs were very dependent on the steric and electrostatic properties of the 5-substituent. This similarity is clearly revealed by the Crystal Packing Similarity method focusing on how much of the coordination sphere can be overlaid and where the packing differs, rather than seeking true isostructurality with emphasis on the unit cell and symmetry. Hence, the fenamate fragment is a polymorphophore in that the fragment does generate a wide range of crystal packings that are reasonably low in energy. However, the specific substituents determine the energy differences between these structures. This can give many structures close enough in energy and different enough in packing to be observed as polymorphs, as seen for TA and ROY, or only one structure (or closely related structures) so that there are no practically important polymorphs, as for FA and presumably the bromo derivative of ROY which has only given one form despite experimental screening.[4]

The considerable similarity in large clusters between some of the known and hypothetical structures of TA, and the closeness of their energies (Figure 7b), also suggests that crystal growth errors are very likely. This could lead to alternative forms of disorder from form V, defects or regions of different

Table 5. Crystal Packing Similarity Comparisons of the Experimental Structures of FA and TA (with Three Ordered Models for Form V) and Their Most Stable Hypothetical Crystal Structures with the Crystal Structures of the Other Fenamates Shown in Figure 1 in the CSD[a]

	n ($rmsd_n$/Å)							
	FPAMCA	FPAMCA11	LAHLOW	PEFMET	PEFNAQ	SURMEY	SURMOI	XYANAC
				FA				
QQQBTY02	2(0.71)	**4(1.33)**	**7(0.84)**	3(1.28)	**6(0.62)**	3(0.5)	3(1.2)	**4(0.49)**
#1FA_22	2(0.41)	**5(1.91)**	**6(1.31)**	2(0.13)	**11(0.96)**	**4(0.98)**	**4(1.08)**	3(1.8)
#2FA_2	2(0.43)	3(0.56)	**7(1.01)**	2(0.1)	**11(0.51)**	3(1.07)	**7(0.98)**	3(0.86)
				TA				
II	1(0.89)	2(0.15)	2(0.59)	2(0.11)	1(0.61)	2(0.12)	**12(1.87)**	2(0.29)
I	2(0.59)	2(0.48)	3(0.61)	1(0.7)	**13(0.38)**	**6(1.78)**	**4(1.2)**	2(0.62)
III	1(0.81)	**7(0.75)**	2(0.48)	**13(0.33)**	2(0.55)	**13(0.61)**	3(0.41)	**13(0.45)**
IV	2(0.87)	**6(0.71)**	3(1.09)	**11(0.49)**	2(0.46)	**13(0.84)**	3(0.56)	**15(0.3)**
V_a	2(0.57)	2(0.46)	**5(0.42)**	1(0.68)	3(0.39)	2(0.22)	2(0.18)	2(0.57)
V_b	2(0.75)	3(0.32)	**7(0.64)**	2(0.47)	**4(1.10)**	**5(0.41)**	**4(1.19)**	**5(0.72)**
V_c	2(0.95)	2(0.84)	**5(0.41)**	1(0.42)	**4(1.10)**	**4(0.51)**	2(0.29)	3(0.46)
#2TA_15	2(0.52)	2(0.53)	3(0.91)	1(0.77)	**14(0.4)**	**4(0.82)**	**4(1.22)**	2(0.7)
#3TA_876	1(0.93)	**4(1.56)**	**7(1.42)**	3(0.43)	1(0.66)	3(0.71)	**4(0.47)**	2(0.37)
#4TA_6243	2(0.54)	3(1.15)	3(1.76)	1(0.69)	**4(0.16)**	**4(1.49)**	2(0.17)	3(0.91)
#6TA_82	1(0.92)	2(0.17)	2(0.61)	2(0.12)	2(0.64)	2(0.08)	**15(0.28)**	2(0.28)

[a]The similarity is given in the form $n(rmsd_n)$, with the overlays of four or more molecules highlighted.

dx.doi.org/10.1021/cg3007348 | *Cryst. Growth Des.* 2012, 12, 4230−4239

polymorphic structures, which are hard to detect even by single crystal diffraction.[71] The powder X-ray similarities of some of the known structures (Table 2) also suggest that detecting whether microcrystalline samples are phase pure is challenging. This adds to the difficulties in experimentally determining the relative stability of the polymorphs (Table 1 and Supporting Information). The accuracy of our calculations, or other methods,[37] is not sufficient for confidence in the relative ordering of the structures within the clusters around the global minima (Supporting Information). However, we can be confident that there is a marked difference in the complexity of the crystallization behavior of TA and FA: their crystal energy landscapes are qualitatively different in the range of structures within the energy range of possible polymorphism or disorder.

5. CONCLUSIONS

Examination of the computer-generated low-energy crystal structures of the unsubstituted structural fragment, fenamic acid, and a derivative, tolfenamic acid, show that all structures are based on the same $R_2^2(8)$ hydrogen bonded dimer, and differ in the packing of the phenyl rings. The conformational flexibility allows a wide variety of interdigitating packings of the phenyl rings (including multiple molecules in the asymmetric unit), which, once formed, are sufficiently kinetically trapped and thermodynamically favorable, to be crystalline polymorphs. In this sense, the fenamate fragment is a polymorphophore, rationalizing the polymorphism of many fenamates. However, it is the phenyl ring substituents that determine the variety of such crystal structures, and their relative energies. In the case of FA, the known and a closely related structure are thermodynamically favored above other alternatives, limiting the range of potential polymorphism. In contrast, the chloro and methyl substituents of TA produce a range of almost equi-energetic packings, including the polymorphs already observed. Hence, the FA fragment is a polymorphophore in that this molecular fragment can pack in a wide range of distinct crystal structures with different conformations that are energetically favorable. However, any substituents have sufficient effect on the packing to determine which structures are the lowest in energy and hence whether the molecule is polymorphic. Thus, molecules containing a "polymorphophore" like the FA fragment are quite likely to have a complex range of polymorphs, but this is not guaranteed because it is so dependent on the interactions between the substituents. This important caveat explains the superficially contradictory observation that the bare polymorphophore, fenamic acid, has no known polymorphs. A molecule-specific crystal energy landscape calculation, which evaluates the effect of the substituents on the intermolecular interactions and the conformational flexibility of the molecule, and the range of structures in which these two balance to give the greatest stability, may well assist in reducing the range of experimental screening required for molecules containing polymorphophores.

■ ASSOCIATED CONTENT

Supporting Information

Discussion of experimental thermodynamic measurements; the disorder in form V; further computational details and comparisons of crystal structures. This material is available free of charge via the Internet at http://pubs.acs.org.

■ AUTHOR INFORMATION

Corresponding Author

*E-mail: s.l.price@ucl.ac.uk.

Notes

The authors declare no competing financial interest.

■ ACKNOWLEDGMENTS

DE Braun for helpful discussion on the thermodynamic data. O.G.U. is financially supported by CCDC and EPSRC GRANT EP/G036675/1 (M3S Centre for Doctoral Training). A.J.C.-C. thanks De Nederlandse Organisatie voor Wetenschappelijk Onderzoek (NWO) for a VENI fellowship, CCDC and PIPMS for funding of part of the work.

■ REFERENCES

(1) Bernstein, J. *Cryst. Growth Des.* **2011**, *11*, 632−650.
(2) Yu, L. *Acc. Chem. Res.* **2010**, *43*, 1257−1266.
(3) Yu, L.; Stephenson, G. A.; Mitchell, C. A.; Bunnell, C. A.; Snorek, S. V.; Bowyer, J. J.; Borchardt, T. B.; Stowell, J. G.; Byrn, S. R. *J. Am. Chem. Soc.* **2000**, *122*, 585−591.
(4) Lutker, K. M.; Tolstyka, Z. P.; Matzger, A. J. *Cryst. Growth Des.* **2008**, *8*, 136−139.
(5) Yang, S. S.; Guillory, J. K. *J. Pharm. Sci.* **1972**, *61*, 26−40.
(6) Rossi, D.; Gelbrich, T.; Kahlenberg, V.; Griesser, U. J. *CrystEngComm* **2012**, *14*, 2494−2506.
(7) Lutker, K. M.; Matzger, A. J. *J. Pharm. Sci.* **2010**, *99*, 794−803.
(8) Arlin, J. B.; Price, L. S.; Price, S. L.; Florence, A. J. *Chem. Commun.* **2011**, *47*, 7074−7076.
(9) Lopez-Mejias, V.; Kampf, J. W.; Matzger, A. J. *J. Am. Chem. Soc.* **2009**, *131*, 4554−4555.
(10) Costantino, L.; Barlocco, D. *Curr. Med. Chem.* **2006**, *13* (1), 65−85.
(11) Lopez-Mejias, V.; Kampf, J. W.; Matzger, A. J. *J. Am. Chem. Soc.* **2012**, *134*, 9872−9875.
(12) Surov, A. O.; Perlovich, G. L. *J. Struct. Chem.* **2010**, *51*, 308−315.
(13) Li, H.; Stowell, J. G.; Borchardt, T. B.; Byrn, S. R. *Cryst. Growth Des.* **2006**, *6*, 2469−2474.
(14) Pagola, S.; Stephens, P. W.; He, X.; Byrn, S. R. *Materials Science Forum,* **2001**, *378−381*, 789−794.
(15) Zhou, T.; Li, F.; Fan, Y.; Song, W.; Mu, X.; Zhang, H.; Wang, Y. *Chem. Commun.* **2009**, 3199−3201.
(16) Murthy, H. M. K.; Bhat, T. N.; Vijayan, M. *Acta Crystallogr. Sect. B* **1982**, *38*, 315−317.
(17) Mei, X. F.; August, A. T.; Wolf, C. *J. Org. Chem.* **2006**, *71*, 142−149.
(18) Mei, X. F.; August, A. T.; Wolf, C. *J. Org. Chem.* **2006**, *71*, 142−149.
(19) Alvarez, A. J.; Singh, A.; Myerson, A. S. *Cryst. Growth Des.* **2009**, *9*, 4181−4188.
(20) Dokorou, V.; Kovala-Demertzi, D.; Jasinski, J. P.; Galani, A.; Demertzis, M. A. *Helv. Chim. Acta* **2004**, *87*, 1940−1950.
(21) Day, G. M. *Crystallogr. Rev.* **2011**, *17*, 3−52.
(22) Bardwell, D. A.; et al. *Acta Crystallogr., Sect. B* **2011**, *67*, 535−551.
(23) Price, S. L. *Acc. Chem. Res.* **2009**, *42*, 117−126.
(24) Kazantsev, A. V.; Karamertzanis, P. G.; Adjiman, C. S.; Pantelides, C. C.; Price, S. L.; Galek, P. T.; Day, G. M.; Cruz-Cabeza, A. J. *Int. J. Pharm.* **2011**, *418*, 168−178.
(25) Mattei, A.; Li, T. L. *Int. J. Pharm.* **2011**, *418*, 179−186.
(26) Braun, D. E.; Karamertzanis, P. G.; Price, S. L. *Chem. Commun.* **2011**, *47*, 5443−5445.
(27) Cruz-Cabeza, A. J.; Karki, S.; Fabian, L.; Friscic, T.; Day, G. M.; Jones, W. *Chem. Commun.* **2010**, *46*, 2224−2226.
(28) Karamertzanis, P. G.; Kazantsev, A. V.; Issa, N.; Welch, G. W. A.; Adjiman, C. S.; Pantelides, C. C.; Price, S. L. *J. Chem. Theory Comput.* **2009**, *5*, 1432−1448.

(29) Issa, N.; Barnett, S. A.; Mohamed, S.; Braun, D. E.; Copley, R. C. B.; Tocher, D. A.; Price, S. L. *CrystEngComm* **2012**, *14*, 2454−2464.
(30) Cruz-Cabeza, A. J.; Day, G. M.; Jones, W. *Phys. Chem. Chem. Phys.* **2011**, *13*, 12808−12816.
(31) Habgood, M. *Cryst. Growth Des.* **2011**, *11*, 3600−3608.
(32) Torrisi, A.; Leech, C. K.; Shankland, K.; David, W. I. F.; Ibberson, R. M.; Benet-Buchholz, J.; Boese, R.; Leslie, M.; Catlow, C. R. A.; Price, S. L. *J. Phys. Chem. B* **2008**, *112*, 3746−3758.
(33) Braun, D. E.; Karamertzanis, P. G.; Arlin, J. B.; Florence, A. J.; Kahlenberg, V.; Tocher, D. A.; Griesser, U. J.; Price, S. L. *Cryst. Growth Des.* **2011**, *11*, 210−220.
(34) Llinas, A.; Goodman, J. M. *Drug Discovery Today* **2008**, *13*, 198−210.
(35) Andersen, K. V.; Larsen, S.; Alhede, B.; Gelting, N.; Buchardt, O. *J. Chem. Soc. Perkin Trans. 2* **1989**, 1443−1447.
(36) Surov, A. O.; Szterner, P.; Zielenkiewicz, W.; Perlovich, G. L. *J. Pharm. Biomed. Anal.* **2009**, *50*, 831−840.
(37) Mattei, A.; Li, T. *Pharm. Res.* **2012**, *29*, 460−470.
(38) Kazantsev, A. V.; Karamertzanis, P. G.; Adjiman, C. S.; Pantelides, C. C.; Price, S. L.; Galek, P. T. A.; Day, G. M.; Cruz-Cabeza, A. J. *Int. J. Pharm.* **2011**, *418*, 168−178.
(39) Frisch, M. J. et al.*Gaussian 03*; Gaussian Inc.: Wallingford, CT, 2004.
(40) *Mercury CSD 2.2 (Build RCS)*; CCDC: Cambridge, 2001−2007, 2009
(41) Bruno, I. J.; Cole, J. C.; Edgington, P. R.; Kessler, M.; Macrae, C. F.; McCabe, P.; Pearson, J.; Taylor, R. *Acta Crystallogr., Sect. B* **2002**, *58*, 389−397.
(42) Karamertzanis, P. G.; Pantelides, C. C. *Mol. Phys.* **2007**, *105*, 273−291.
(43) Schmidt, M. W.; Baldridge, K. K.; Boatz, J. A.; Elbert, S. T.; Gordon, M. S.; Jensen, J. H.; Koseki, S.; Matsunaga, N.; Nguyen, K. A.; Su, S.; Windus, T. L.; Dupuis, M.; Montgomery, J. A. *J. Comput. Chem.* **1993**, *14*, 1347−1363.
(44) Williams, D. E. *J. Comput. Chem.* **2001**, *22*, 1154−1166.
(45) Stone, A. J. *J. Chem. Theory Comput.* **2005**, *1*, 1128−1132.
(46) Price, S. L.; Leslie, M.; Welch, G. W. A.; Habgood, M.; Price, L. S.; Karamertzanis, P. G.; Day, G. M. *Phys. Chem. Chem. Phys.* **2010**, *12*, 8478−8490.
(47) Cox, S. R.; Hsu, L. Y.; Williams, D. E. *Acta Crystallogr., Sect A* **1981**, *37*, 293−301.
(48) Williams, D. E.; Cox, S. R. *Acta Crystallogr., Sect. B* **1984**, *40*, 404−417.
(49) Coombes, D. S.; Price, S. L.; Willock, D. J.; Leslie, M. *J. Phys. Chem.* **1996**, *100*, 7352−7360.
(50) Kazantsev, A. V.; Karamertzanis, P. G.; Adjiman, C. S.; Pantelides, C. C. *J. Chem. Theory Comput.* **2011**, *7*, 1998−2016.
(51) Kazantsev, A. V.; Karamertzanis, P. G.; Adjiman, C. S.; Pantelides, C. C. In *Molecular System Engineering*; WILEY-VCH Verlag GmbH & Co.: Weinheim, 2010; pp 1−42.
(52) Cossi, M.; Scalmani, G.; Rega, N.; Barone, V. *J. Chem. Phys.* **2002**, *117*, 43−45.
(53) Cooper, T. G.; Hejczyk, K. E.; Jones, W.; Day, G. M. *J. Chem. Theory Comput.* **2008**, *4*, 1795−1805.
(54) Chisholm, J. A.; Motherwell, S. *J. Appl. Crystallogr.* **2005**, *38*, 228−231.
(55) Macrae, C. F.; Edgington, P. R.; McCabe, P.; Pidcock, E.; Shields, G. P.; Taylor, R.; Towler, M.; van de Streek, J. *J. Appl. Crystallogr.* **2006**, *39*, 453−457.
(56) van Mourik, T.; Karamertzanis, P. G.; Price, S. L. *J. Phys. Chem.A* **2006**, *110*, 8−12.
(57) de Gelder, R.; Wehrens, R.; Hageman, J. A. *J. Comput. Chem.* **2001**, *22*, 273−289.
(58) van de Streek, J.; Motherwell, S. *Acta Crystallogr., Sect. B* **2005**, *61*, 504−510.
(59) Desiraju, G. R. *Cryst. Growth Des.* **2008**, *8*, 3−5.
(60) Bhatt, P. M.; Desiraju, G. R. *Chem. Commun.* **2007**, 2057−2059.
(61) Habgood, M.; Grau-Crespo, R.; Price, S. L. *Phys. Chem. Chem. Phys.* **2011**, *13*, 9590−9600.
(62) Gavezzotti, A. *J. Am. Chem. Soc.* **1983**, *105*, 5220−5225.
(63) Lancaster, R. W.; Karamertzanis, P. G.; Hulme, A. T.; Tocher, D. A.; Lewis, T. C.; Price, S. L. *J. Pharm. Sci.* **2007**, *96*, 3419−3431.
(64) Desiraju, G. R. *CrystEngComm* **2007**, *9*, 91−92.
(65) Anderson, K. M.; Steed, J. W. *CrystEngComm* **2007**, *9*, 328−330.
(66) Mahlin, D.; Ponnambalam, S.; Hockerfelt, M. H.; Bergstrom, C. A. S. *Mol. Pharmaceutics* **2011**, *8*, 498−506.
(67) Yu, L.; Reutzel-Edens, S. M.; Mitchell, C. A. *Org. Process Res.Dev.* **2000**, *4*, 396−402.
(68) Barnett, S. A.; Johnson, A.; Florence, A. J.; Price, S. L.; Tocher, D. A. *Cryst. Growth Des.* **2008**, *8*, 24−36.
(69) Mohamed, S.; Barnett, S. A.; Tocher, D. A.; Shankland, K.; Leech, C. K.; Price, S. L. *CrystEngComm* **2008**, *10*, 399−404.
(70) Barnett, S. A.; Hulme, A. T.; Issa, N.; Lewis, T. C.; Price, L. S.; Tocher, D. A.; Price, S. L. *New J. Chem.* **2008**, *32*, 1761−1775.
(71) Bond, A. D. *CrystEngComm* **2012**, *14*, 2363−2366.